BULLETIN OF THE POLISH ACADEMY OF SCIENCES
TECHNICAL SCIENCES, Vol. 71(1), 2023, Article number: e144576
DOI: 10.24425/bpasts.2023.144576

Probabilistic estimation of diverse soil condition impact on vertical axis tank deformation

Kamil ŻYLIŃSKI[1,2] **and Jarosław GÓRSKI**[1]*

[1] Faculty of Civil and Environmental Engineering, Gdańsk University of Technology, Poland
[2] ERSYS, Poland

Abstract. The calculations of fuel tanks should take into account the geometric imperfections of the structure as well as the variability of the material parameters of the foundation. The deformation of the tank shell can have a significant impact on the limit state of the structure and its operating conditions. The paper presents a probabilistic analysis of a vertical-axis, floating-roof cylindrical shell of a tank with a capacity of 50000 m^3 placed on stratified soil with heterogeneous material parameters. The impact of a random subsoil description was estimated using the Point Estimated Method (PEM). In this way, the number of analyzed FEM models was significantly reduced. This approach also makes it possible to assess the sensitivity of tank settlement and deformation to the changing foundation conditions.

Key words: storage tanks; foundation settlement; subsoil parameters; Point Estimated Method.

1. INTRODUCTION

The design of fuel tanks is usually based on a deterministic analysis of ideal models. The calculations ignore both the geometrical and material imperfections of the structure, as well as other factors such as post-welding stresses [1]. The effect of the tank foundation settlement, which may lead to limit state exceedance should be also taken into account [2–5]. Due to the random nature of material parameters, probabilistic methods are commonly used. Depending on the analyzed problem, both the bearing capacity of the foundation in limit states (ULS) and the exceeding of the permissible settlement (SLS) are calculated. A review of the methods allowing us to estimate the reliability of the structure (SRA) and the stochastic finite element method (SFEM), covering both technological and application issues, is presented, e.g., in [6, 7]. Reliability estimation is also included in Eurocodes [8, 9].

Random fields are increasingly used in geotechnical engineering [10–12]. In the calculations, due to the high variability and randomness of the subsoil features, in situ studies are often used [13, 14]. In this way, it is possible to implement probabilistic methods in geotechnical design (due to the amount of data) in accordance with the approach of the philosophy of geotechnical design [15]. As an alternative solution, the soil medium is homogenized [16]. Most often, due to the limited measurement data, the soil stratification and its material parameters are assumed a priori. This approach justifies the introduction of data random distributions that facilitate taking into account the uncertainty in the FEM model.

The paper attempts to describe the subsoil of a fuel tank of a vertical axis, with a floating roof. The calculations are restricted to the estimation of the impact of diverse soil conditions on the tank shell deformation. The effect of geometric and material imperfections is neglected. Non-uniform settlement may subsequently produce excessive tank deformation and operational difficulties, e.g., by floating roof locking. On-site tests make it possible to realistically reflect complex soil conditions and parameter dispersion.

A random description of the structure and material parameters of the soil medium was adopted in the calculations. A spatial random model of the subsoil was used, presented in [17–19]. Complicated random fields were replaced with a simplified discrete model related directly to the finite element pattern. The adoption of an appropriate number of random variables, e.g. Young's modules assigned to individual areas allows us to obtain a realistic dispersion of the results. The created calculation algorithm enables us to use any FEM program.

Point Estimated Method (PEM) [20] was used in the probabilistic analysis. Its optimized versions allow for an effective reduction of the number of samples [21, 22]. The method is often used in the analysis of geotechnical problems [13, 22–24]. The axisymmetric of the tank model and its foundation facilitate a further reduction in the number of samples used in the analysis.

The proposed algorithm combining the simplified random FEM model of the soil medium with the calculations made with the use of PEM can be directly used as a supplement to the deterministic analysis of fuel tanks.

All the computations were performed in the ZSoil environment [25–27] and Python modules [28].

2. FEM MODEL OF A FUEL TANK

This paper analyzes a vertical-axis cylindrical fuel tank with a floating roof (Fig. 1) of a 50000 m^3 volume. The tank diameter is 60.5 m, and its height is 22.0 m. The S355J2 steel was

*e-mail: jgorski@pg.edu.pl

Manuscript submitted 2022-06-27, revised 2022-12-18, initially accepted for publication 2022-12-19, published in February 2023.

assumed for the structure. The numerical model incorporates the sheet thicknesses t_{efect} reduced by corrosion (Table 1). The reduction of the structural stiffness made also an indirect impact on initial imperfections, sheet fabrication tolerances, post-welding stresses, and other means. The mean Young's modulus $E = 210$ GPa and the Poisson's ratio $\nu = 0.3$ were taken for the analysis. The corner ring fixed 0.25 m below the shell top edge was designed in the form of a panel 0.36 m thick.

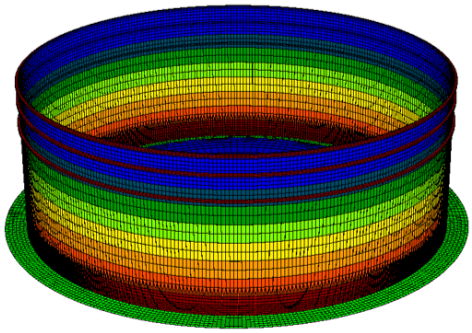

Fig. 1. The tank FEM model (ZSoil)

Table 1
The thicknesses and heights of the tank sections

No.	t_{init} [mm]	t_{efect} [mm]	h [m]	$h_{overall}$ [m]
9	11	7.5	2.25	2.25
8	11	7.5	2.25	4.50
7	12	8.5	2.25	6.75
6	15	11.4	2.50	9.25
5	18	14.4	2.50	11.75
4	21	17.4	2.50	14.25
3	24	20.4	2.50	16.75
2	27	23.2	2.50	19.25
1	30	26.2	2.75	22.00

Shell weight was assumed in the form of nodal loads of 12.04 kN. The tank is filled in with a liquid of density 1000 kg/m^3 up to the level of 19.6 m from the bottom, yielding appropriate hydrostatic pressure. The uniform pressure on the tank bottom corresponds to the liquid pressure. Other loads such as wind pressure and snow effects have not been included [17, 18].

Two different FEM models of the tank subsoil have been developed. The first model was directly related to the axisymmetric FEM model of the tank. The second model is more universal in nature and facilitates the application of probabilistic methods.

3. AXISYMMETRIC MODEL OF TANK FOUNDATION

In situ tests showed a different distribution of the soil parameters in the area of the tank foundation and a complicated layering. As a result of the conducted averaging, five different groups of Young's modulus were identified (Case 1), presented in Fig. 2 and described in Table 2, utilizing the mean value E_{KZ} and the standard deviation σ_{KZ} [17,18]. Note the large values of the variability $\mu_{KZ} = \sigma_{KZ}/E_{KZ}$, reaching even $\mu_{KZ} = 0.86$ for KZ3. The dispersion of Young's modulus indicates the random nature of the analyzed problem.

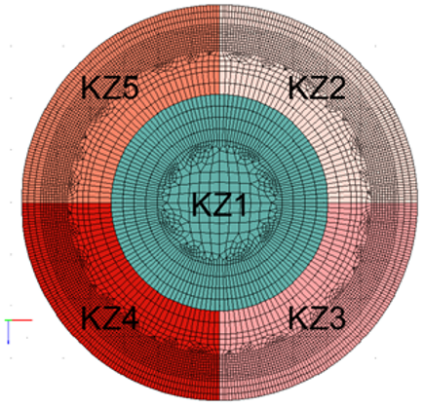

Fig. 2. The subsoil strata distributions (Case 1)

Table 2
Material parameters of subsoil strata

	KZ1	KZ2	KZ3	KZ4	KZ5
E_{KZ} [MPa]	39.92	38.54	43.40	35.30	37.57
σ_{KZ} [MPa]	10.30	10.94	37.22	10.74	10.59
μ_{KZ} [–]	0.26	0.28	0.86	0.30	0.28

The soil strata and tank foundation have been described by eight-node 3D elements. (Fig. 3).

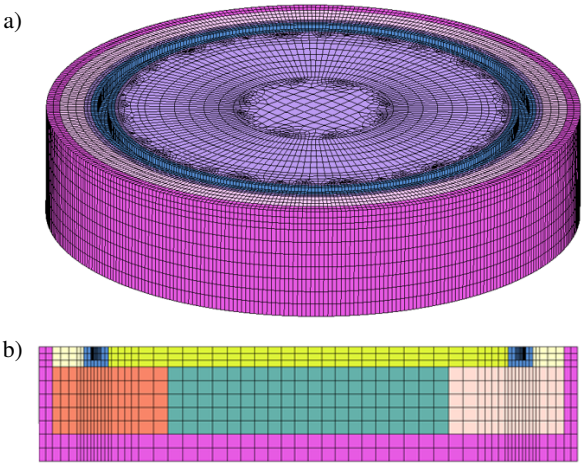

Fig. 3. Three-dimensional overview of a tank: a) foundation section, b) subsoil section (ZSoil)

The foundation ring strip was modeled as a reinforcement element (RC) whose dimensions are 4.05 × 3.0 m (Fig. 3). The transfer of friction forces between the tank sheet, the soil, and the concrete foundation strip was considered by the contact

elements with friction coefficients $\mu = 0.3$. The soil regions of the footing (Table 2) are presented in Fig. 3b in orange, green, and pink. The yellow elements between the foundation strip and the external area correspond to the soil parameters denoted by $E = 128$ MPa. The stiffness modulus of concrete mixed with sand (marked in greenish, Fig. 3) is described by a value $E = 130$ MPa. The boundary elements of the subsoil (marked in violet, Fig. 3) form a layer whose Young's modulus is $E = 50$ MPa. The value has been numerically determined to consider the deformation impact of an infinite zone [17, 18].

The first approach distinguishes five subregions *KZ*1-*KZ*5 based on the data included in Table 2. The model presented in Fig. 2 yields deformation of the bottom central node $u_5 = 0.066$ m (5 is the number of distinctly assumed material parameters). While the parameters *KZ* of all regions are averaged to a single value $KZ = 38.95$ MPa, the maximum settlement of the bottom raises to $u_1 = 0.069$ m.

The next step addresses the impact of stiffness modulus *KZ* variation according to Table 3. The test is aimed at determining the relationship type between the soil stiffness variation and the mechanical response of the tank.

Table 3
Material parameters of subsoil strata

No.	E_{mean} [MPa]	Sensitivity analysis [MPa]			
		$+0.1\sigma_E$	$+0.4\sigma_E$	$-0.1\sigma_E$	$-0.4\sigma_E$
KZ1	42.71	46.99	59.80	38.44	25.63
KZ2	37.19	40.91	52.07	33.47	22.32
KZ3	41.23	45.36	57.73	37.11	24.74
KZ4	38.12	41.93	53.37	34.31	22.87
KZ5	39.98	43.97	55.97	35.98	23.99

The sensitivity analysis of two parameters was performed, i.e., settlement of the center point of the tank bottom and deformation of the tank shell at the contact with the ring foundation. The latter parameter is calculated as the average of all vertical displacements of the annular plate. The relation between the assumed moduli *KZ*1÷*KZ*2 and the vertical displacement u_y is presented in Fig. 4. They indicate a significant non-linear effect of changes in material parameters on bottom settling and a smaller impact on the deformation of the tank shell edge.

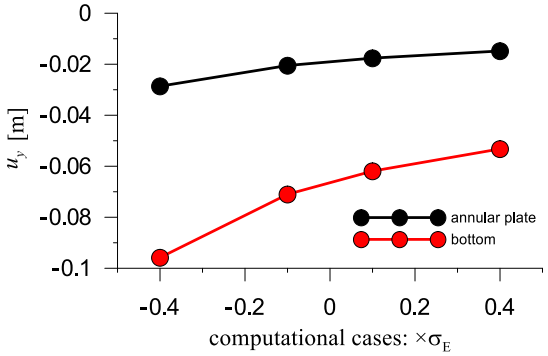

Fig. 4. The relationship – deflections vs variable subsoil stiffness

Both the assumed foundation areas (Figs. 2 and 3) and the material parameters (Table 2) are random. Their precise determination is usually not possible due to the limited testing performed on the construction site. The adoption of the axisymmetric description of the soil parameter distributions (Fig. 2) results only from the facilitation of FEM modeling and does not reflect the real nature of the foundation. This is a limitation in the case of a random description of the subsoil.

4. A RANDOM DESCRIPTION OF SUBSOIL PARAMETERS

In [19], a simplified algorithm describing soil parameters diversion and their stratification in the area of the structure foundation was proposed. Parametric calculations were made using the FEM model of an indirectly loaded cube-shaped subsoil with the dimension $10 \times 10 \times 10$ m (1000 finite elements). In subsequently analyzed models, a different number of random variables n_E ($1 \leq n_E \leq 1000$) was assumed to describe the soil stiffness module variability. It was found that the expected value of soil settlement remains practically unchanged. However, the standard deviation of these quantities varies considerably. By introducing a normalizing parameter $\ln(n_E)$ characterizing the division of the FEM model into a finite element, a linear relationship was obtained between the FEM structure description and the results estimating the settlement standard deviation. The algorithm proposed in [19] can therefore be directly applied in the analysis of the foundation of fuel tanks.

Two models were adopted resulting from the division of the foundation area into $2 \times 2 = 4$ (Case 2) and $3 \times 3 = 9$ (Case 3) zones (Fig. 5). The division into finite elements with assigned

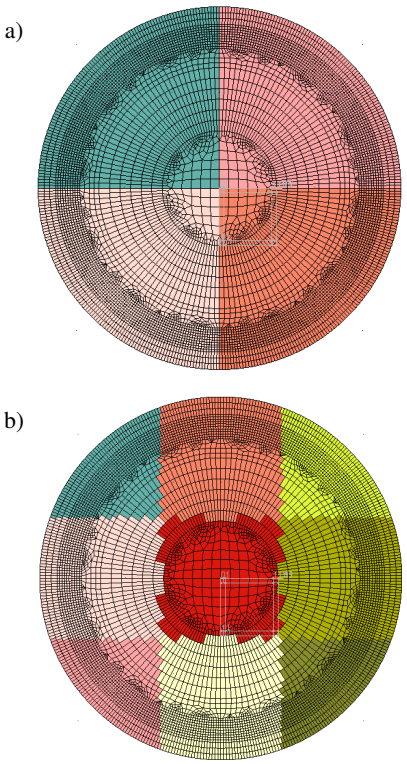

Fig. 5. Division of the reservoir foundation area into a) four (Case 2) and b) nine sub-areas (Case 3)

different material parameters is made automatically with the use of proprietary software.

The soil material parameters were defined on the basis of the data in Table 2. It was assumed that Young's modulus can be described by a normal distribution with a mean value $\hat{E} = 39.85$ MPa and standard deviation $\hat{\sigma}_E = 11.96$ MPa (coefficient of variation $\hat{v}_E = 0.3$). Assuming the standard deviation, the maximum variability of $\mu_{KZ} = 0.86$ was not taken into account (Table 2). The adopted description of the dispersion of soil parameters allows for the full application of the probabilistic analysis.

5. PROBABILISTIC ANALYSIS

Probabilistic analysis requires the adoption of an appropriate calculation method. The simplest possible and the most universal is the Monte Carlo (MC) method. However, in the case of the analyzed tank, the computation time of a single model is too long and makes it impossible to perform the necessary tens or even hundreds of MC calculations. Estimation of probabilistic measures of the tank response was performed using the Point Estimated Method (PEM). In its standard form [20], calculations should be made for n^2 samples, where n is the number of random variables. It should be noted that the distributions of input random variables do not need to be given because only the first two moments should be adopted. In [29], an algorithm was proposed that allows us to reduce the number of samples to $2n+1$.

In the case of the tank analysis, the limit state function $Y = f(E_1, E_2, E_n)$ is not given explicitly. The values of the function Y can be obtained using any deterministic finite element program, e.g., ZSoil. First, the calculations are performed for an ideal model where all random variables (Young's modulus) are described by their mean values [29]:

$$y_0 = f(\hat{E}_1, \hat{E}_2, \ldots, \hat{E}_n). \tag{1}$$

Next, two values shifted from the mean values by $\pm\sigma_{E_i}$ are calculated for each random variable:

$$y_i^{-/+} = f\left(\hat{E}_1, \hat{E}_2, \ldots \hat{E}_i \mp \hat{\sigma}_{E_i} \ldots, \hat{E}_n\right). \tag{2}$$

On this basis, the following parameters are defined:

$$\overline{y}_j = \frac{y_i^+ + y_i^-}{2}, \tag{3}$$

$$V_{y_j} = \frac{y_i^+ - y_i^-}{y_i^+ + y_i^-}. \tag{4}$$

Finally, the mean value $\overline{Y}$ and the coefficient of variations v_Y are determined:

$$\overline{Y} = y_0 \prod_{i=1}^{n} \left(\frac{\overline{y}_i}{y_0}\right), \tag{5}$$

$$v_Y = \sqrt{\left\{\prod_{i=1}^{n}\left(1 + V_{y_i}^2\right)\right\} - 1}. \tag{6}$$

In the case of the analyzed tank foundation, the number of PEM samples can be reduced by taking into account the axisymmetric conditions. All areas (Figs. 2 and 4) are described by one Young's modulus defined by the expected value $\hat{E} = 39.85$ MPa and standard deviation $\hat{\sigma}_E = 11.96$ MPa. However, it is assumed that individual areas of soil may have different material parameters. Thus, in the case of the schemes presented in Figs. 2 and 5, five (Case 1), four (Case 2) and nine (Case 3) random variables described with the same distribution were assumed, respectively. As a result of using this approach, the number of required calculations is reduced to three samples for the scheme from Fig. 2, and two and four samples for the scheme from Fig. 5a and Fig. 5b.

Analysis of the settlement impact on the tank shape deformation requires an appropriate definition of the output results. The following two parameters were selected:

- The vertical displacement of the middle node of the bottom u_{botom}.
- The deformation of the annular plate u_{ann} associated with the ring foundation settlement, determined as the average value of all vertical displacements of the plate finite element nodes.

The calculation results for Case 1 and Case 2 (ZSoil) are presented in Table 4, and for Case 3 in Table 5. Note that due to the axial symmetry, the calculations are performed for a quarter of the FEM model, i.e. middle and corner sections. In this way, a significant saving of computational time was achieved.

Table 4
FEM calculation results: Case 1 and Case2

Case		Case 1				Case 2	
Varying part		Middle section		Corner section		Corner section	
E value	$\hat{E}$	$\hat{E}+\hat{\sigma}_E$	$\hat{E}-\hat{\sigma}_E$	$\hat{E}+\hat{\sigma}_E$	$\hat{E}-\hat{\sigma}_E$	$\hat{E}+\hat{\sigma}_E$	$\hat{E}-\hat{\sigma}_E$
u_{bottom} [m]	–0.069	–0.054	–0.068	–0.074	–0.084	–0.065	–0.064
u_{ann} [m]	–0.018	–0.018	–0.018	–0.020	–0.019	–0.020	–0.018

Table 5
FEM calculation results – Case 3

Varying part		Middle section		Middle up section		Corner section	
E value	$\hat{E}$	$\hat{E}+\hat{\sigma}_E$	$\hat{E}-\hat{\sigma}_E$	$\hat{E}+\hat{\sigma}_E$	$\hat{E}-\hat{\sigma}_E$	$\hat{E}+\hat{\sigma}_E$	$\hat{E}-\hat{\sigma}_E$
u_{bottom} [m]	–0.069	–0.064	–0.065	–0.055	–0.055	–0.064	–0.065
u_{ann} [m]	–0.018	–0.018	–0.019	–0.018	–0.018	–0.018	–0.019

The calculations made with the use of PEM are shown in Table 6. The displacement expected value $\hat{u}$, coefficient of variations $\hat{v}$ (formulas (5) and (6)), and standard deviation $\hat{\sigma}_u = \hat{v}\hat{u}$

were estimated. By analyzing the results presented in Table 6, it can be concluded that the determined expected values and standard deviations of displacements for different models differ significantly. Due to the overestimated values of the coefficient of variations, the model with four variables (Case 1) is overly simplified. Case 2 and Case 3 models are different in nature and should not be directly compared. Nevertheless, the analysis confirms the necessity to use probabilistic methods in cases for which the distribution and material parameters of individual areas of the substrate are not sufficiently specified.

Table 6
PEM calculation results

	Case 1 (Fig. 2)	Case 2 (Fig. 5a)	Case 3 (Fig. 5b)
$\hat{u}_{\text{bottom}}$ [m]	–0.052	–0.076	–0.020
$\hat{v}_{\text{bottom}}$	0.219	0.077	0.010
$\hat{\sigma}_{\text{bottom}}$ [m]	0.011	0.006	0.0002
$\hat{u}_{\text{ann}}$ [m]	–0.022	–0.020	–0.018
$\hat{v}_{\text{ann}}$	0.111	0.021	0.059
$\hat{\sigma}_{\text{ann}}$ [m]	0.002	0.0004	0.011

The PEM method also facilitates obtaining information about the impact of changing the parameters assigned to particular soil areas on the deformation of the tank. Using the results of calculations for Case 2 (5 variables), Fig. 6 presents the analysis of the displacement of the middle point of the bottom of the tank, and Fig. 7 shows the mean of displacements of the tank annular plate. In the first case, changes in Young's modulus of the subsoil central part cause a significant change in the displacement u_{bottom}. But in the case of changing stiffness in one of the corner zones the change is small. In the case of the analysis of annular plate u_{ann} displacements, none of the elements (middle or corner) has a major impact on the obtained results. A sample of the global deformation of the shell and the subsoil is presented in Fig. 8.

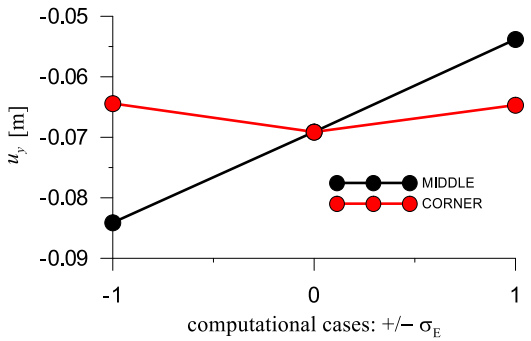

Fig. 6. Sensitivity analysis – Case 1 – bottom of the tank

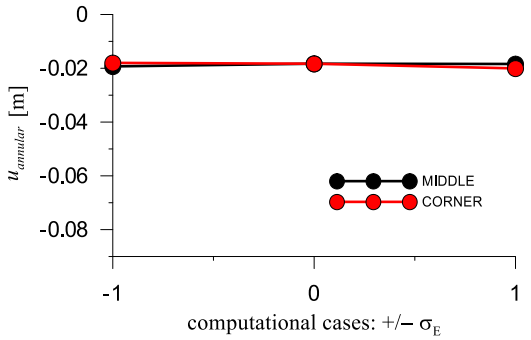

Fig. 7. Sensitivity analysis – Case 1 – annular plate

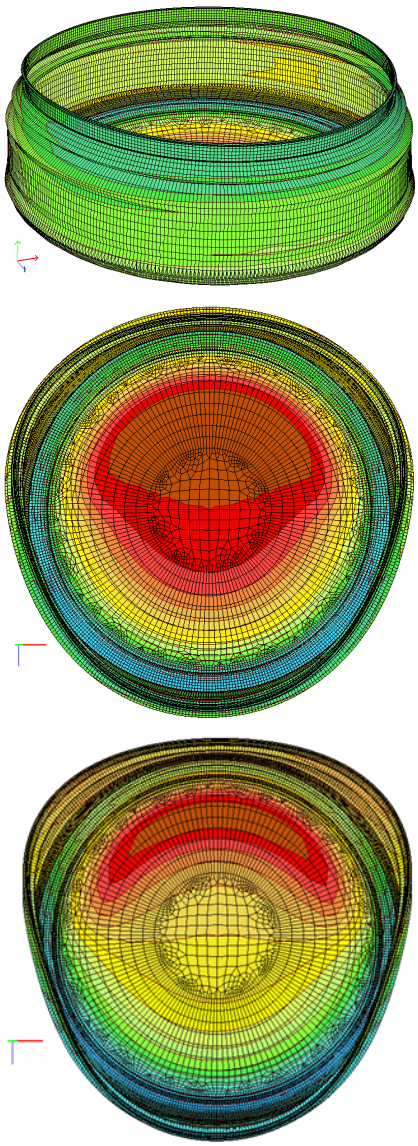

Fig. 8. The map of nodal deflections (Case 2)

6. CONCLUSIONS

The paper shows that by using simplified FEM models and the PEM algorithm, it is possible to analyze the influence of various material parameters of the foundation on the deformation of the tank structure. The conducted tests show that the structure exhibits slight deformation due to subsoil stiffness degradation. However, a full assessment of the impact of the non-uniform tank settlements on the locking of the guides of a floating roof

or failure of the tank equipment can only be made after a comprehensive analysis of tank shell deformation.

The results of numerical calculations should be also verified with measurements made on a real object, e.g. [30]. The impact of the tank geometry imperfections or other in-situ aspects may lead to different results and conclusions.

REFERENCES

[1] K. Rasiulis, A. Šapalas, R. Vadlūga, and M. Samofalov. "Stress/strain state investigations for extreme points of thin wall cylindrical tanks," *J. Constr. Steel. Res.*, vol. 62, pp. 1232–1237, 2006, doi: 10.1016/j.jcsr.2006.04.016.

[2] G. Grget, K. Ravnjak, and A. Szavits-Nossan, "Analysis of results of molasses tanks settlement testing," *Soils Found.*, vol. 58, pp. 1260–1271, 2018, doi: 10.1016/j.sandf.2018.07.009.

[3] S. Gunerathne, H. Seo, W.D. Lawson, and P.W. Jayawickrama, "Analysis of edge-to-center settlement ratio for circular storage tank foundation on elastic soil," *Comput. Geotech.*, vol. 102, pp. 136–147, 2018, doi: 10.1016/j.compgeo.2018.05.008.

[4] R. Ignatowicz and E. Hotala, "Failure of cylindrical steel storage tank due to foundation settlements," *Eng. Fail. Anal.*, vol. 115, 2020, doi: 10.1016/j.engfailanal.2020.104628.

[5] S. Nassernia and H. Showkati, "Experimental investigation to local settlement of steel cylindrical tanks with constant and variable thickness," *Eng. Fail. Anal.*, vol. 118, 2020, doi: 10.1016/j.engfailanal.2020.104916.

[6] W. Puła and Ł. Zaskórski, "On some methods in safety evaluation in geotechnics," *Stud. Geotech. Mech.*, vol. 37, no. 2, pp. 17–32, 2015, doi: 10.1515/sgem-2015-0016.

[7] M. Aldosary, J. Wang, and C. Li, "Structural reliability and stochastic finite element methods: State-of-the-art review and evidence-based comparison," *Eng. Comput.*, vol. 35, pp. 2165–2214, 2018, doi: 10.1108/EC-04-2018-0157.

[8] B.K. Low and K.K. Phoon, "Reliability-based design and its complementary role to Eurocode 7 design approach," *Comput. Geotech.*, vol. 65, pp. 30–44, 2015, doi: 10.1016/j.compgeo.2014.11.011.

[9] K.K. Phoon *et al.*, "Some observations on ISO2394:2015 Annex D (Reliability of Geotechnical Structures)," *Struct. Saf.*, vol. 62, pp. 24–33, 2016, doi: 10.1016/J.STRUSAFE.2016.05.003.

[10] G.A. Fenton and D.V. Griffiths, "Three-Dimensional Probabilistic Foundation Settlement," *J. Geotech. Geoenvironmental Eng.*, vol. 131, pp. 232–239, 2005, doi: 10.1061/(asce)1090-0241(2005)131:2(232).

[11] W. Puła and M. Chwała, "Random bearing capacity evaluation of shallow foundations for asymmetrical failure mechanisms with spatial averaging and inclusion of soil self-weight," *Comput. Geotech.*, vol. pp. 101, 176–195, 2018, doi: 10.1016/j.compgeo.2018.05.002.

[12] T. Al-Bittar, A.-H. Soubra, and J. Thajeel, "Kriging-based reliability analysis of strip footings resting on spatially varying soils," *J. Geotech. Geoenvironmental Eng.*, vol. 144, p. 04018071, 2018, doi: 10.1061/(asce)gt.1943-5606.0001958.

[13] R. Suchomel and D. Mašín, "Probabilistic analyses of a strip footing on horizontally stratified sandy deposit using advanced constitutive model," *Comput. Geotech.*, vol. 38, pp. 363–374, 2011, doi: 10.1016/j.compgeo.2010.12.007.

[14] Z. Młynarek, J. Wierzbicki, and P. Monaco, "Use of DMT and CPTU to assess the G_0 profile in the subsoil," In: *Cone Penetration Testing 2022*, G. Gottardi and L. Tonii, Eds., Taylor& Francis Group, CRC Press 2022, pp. 570–576, doi: 10.1201/9781003308829-82.

[15] T. Godlewski and W. Bogusz, "Philosophy of geotechnical design in civil engineering – Possibilities and risks," *Bull. Pol. Acad. Sci. Tech. Sci.*, vol. 67, no 2, pp. 289–306, 2019, doi: 10.24425/bpas.2019.128258.

[16] J. Ching, Y.G. Hu, and K.K. Phoon, "Effective Young's modulus of a spatially variable soil mass under a footing," *Struct. Saf.*, vol 73, pp. 99–1132, 2018, doi: 10.1016/j.strusafe.2018.03.004.

[17] K. Żyliński and J. Górski, "Deformation of a shell of a fuel tank caused by non-uniform soil settlement," in *XXVII LSCE 2021 Lightweight Structures in Civil Engineering. Contemporary problems. Book of Abstracts*, J. Szafran and M. Kamiński, Eds., Poland, 2021, pp. 161–164.

[18] K. Żyliński and J. Górski, "The impact of footing conditions of a vertical-axis floating-roof tank on structural shell deformation," in *XXVII LSCE 2021 Lightweight Structures in Civil Engineering. Contemporary problems. Book of Abstracts*, J. Szafran and M. Kamiński, Eds., Poland, 2021.

[19] K. Żyliński, K. Winkelmann, and J. Górski, "The effect of the selection of 3-D random numerical soil models on strip foundation settlements," *Appl. Sci.*, vol. 11, 2021, doi: 10.3390/app11167293.

[20] E. Rosenblueth, "Point estimates for probability moments," *Proc. Natl. Acad. Sci. USA*, vol. 72, pp. 3812–3814, 1975, doi: 10.1073/pnas.72.10.3812.

[21] M.E. Harr, "Probabilistic estimates for multivariate analyses," *Appl. Math. Model*, vol. 13, pp. 313–318, 1989, doi: 10.1016/0307-904X(89)90075-9.

[22] H.P. Hong, "An efficient point estimate method for probabilistic analysis," *Reliab. Eng. Syst. Saf.*, vol. 59, pp. 261–267, 1998, doi: 10.1016/S0951-8320(97)00071-9.

[23] M. Ahmadabadi and R. Poisel, "Assessment of the application of point estimate methods in the probabilistic stability analysis of slopes," *Comput. Geotech.*, vol. 69, pp. 540–550, 2015, doi: 10.1016/j.compgeo.2015.06.016.

[24] J.P. Wang and D. Huang, "Rosen point: A Microsoft Excel-based program for the Rosenblueth point estimate method and an application in slope stability analysis," *Comput. Geosci.*, vol. 48, pp. 239–243, 2012, doi: 10.1016/j.cageo.2012.01.009.

[25] S. Commend, S. Kivell, R. Obrzud, K. Podleś, A. Truty, and T. Zimmermann, *Computational geomechanics. getting started with ZSOIL.PC.* V. Rossolis Editions, Switzerland: Preverenges 2018.

[26] A. Truty, "On consistent nonlinear analysis of soil-structure interaction problems," *Stud. Geotech. Mech.*, vol. 40, no. 2, pp. 86-95, 2018, doi: 10.2478/sgem-2018-0019.

[27] T. Zimmermann, J. Sarf, A. Truty, and K. Podles, "Numerics for geotechnics and structures. Recent developments in ZSoil.PC," in *Applications of Computational Mechanics in Geotechnical Engineering V*; Taylor & Francis. 2007, doi: 10.1201/9781439833414.ch8.

[28] Python Manual – 2.7.17, 2019.

[29] A.S. Nowak and K.R. Collins, *Reliability of structures*, New York 2000.

[30] W. Bogusz and M. Kociniak, "Numerical analysis of a foundation of a cooling tower in difficult geotechnical conditions," *Proc. of the 9th European Conference on Numerical Methods in Geotechnical Engineering (NUMGE 2018)*, A.S. Cardoso, J.L. Borges, P.A. Costa, A.T. Gomes, J.C. Marques and C.S. Vieira, Eds., Portugal, pp. 919–926, 2018.